



# Nanohertz gravitational waves from supergravity inflationary model with double-inflection-point

Tie-Jun Gao<sup>1,a</sup>, Ke-Sheng Sun<sup>2</sup>, Xiu-Yi Yang<sup>3</sup>

<sup>1</sup> School of Physics, Xidian University, Xi'an 710071, China

<sup>2</sup> Department of Physics, Baoding University, Baoding 071000, China

<sup>3</sup> School of science, University of Science and Technology Liaoning, Anshan 114051, China

Received: 28 November 2023 / Accepted: 14 February 2024 / Published online: 26 February 2024  
© The Author(s) 2024

**Abstract** Recently, the worldwide pulsar timing array(PTA) collaborations, such as the Chinese Pulsar Timing Array (CPTA), the European PulsarTiming Array (EPTA), the North American Nanohertz Observatory for Gravitational Waves (NANOGrav) and the Parkers Pulsar Timing Array (PPTA) published the analysis of PTA data, which is consistent with the Hellings–Downs curve, thus provides evidence for the existence of stochastic gravitational wave backgrounds (SGWB). In this paper, we will show that such SGWB signal observed by PTA can be explained by the gravitational waves (GWs) induced from double-inflection-point inflationary model in the framework of supergravity with a single chiral superfield. In this model, one of the inflection points leads to a large peak in the scalar power spectrum at small scales, and when this peak re-enters the horizon, it will induce GWs with the frequencies around nanohertz. In addition, we show that the high-density regions corresponding to the peak can collapse into planet-mass primordial black holes (PBHs), thus act as a component of dark matter (DM).

## 1 Introduction

Recently, the worldwide pulsar timing array(PTA) collaborations, such as the Chinese Pulsar Timing Array (CPTA) [1], the European Pulsar Timing Array (EPTA) [2,3], the North American Nanohertz Observatory for Gravitational Waves(NANOGrav) [4–6] and the Parkers Pulsar Timing Array (PPTA) [7,8] published their results, announced that a common-spectrum signal consistent with the Hellings–Downs spatial correlations [9] has been observed, which is strong evidence for a stochastic gravitational wave backgrounds(SGWB).

The nanohertz gravitational wave (GW) signals may originate from the early universe, such as a slight first-order phase transition after the end of double field inflation [10], or the QCD phase transition after inflation [11,12],etc. The GW signals can also be induced by scalar perturbations during inflation, if the scalar power spectrum has a large peak at low scales, when the peak re-enters the horizon, it will induce GWs. Such enhancement of the power spectrum can be achieved from the ultra-slow-roll phase during inflation [13–17], or the framework of effective field theory [18], or the non-standard kinetic terms in string theory [19]. In this work, we will focus on the ultra-slow-roll phase near the inflection point from supergravity models.

Although the inflation of the early universe has been confirmed by a large number of observations, such as WMAP [20] and Planck collaboration [21], but the physical origin of inflation is not clear. A feasible model building scheme is to study the inflationary models in the framework of supergravity [22–28]. However, since the F-term potential of supergravity contains the exponential factor  $e^{|\Phi|^2}$ , which will make the slow-roll parameter  $\eta$  extremely large and thus destroy the slow roll condition, this is called the  $\eta$  problem [28]. One solution to this problem is to introduce additional chiral superfields [29,30]. Another way is to use a single chiral superfield, and add a quartic term in the Kähler potential [31,32]. So in this work, we will consider a double-inflection-point inflationary model realized in the framework of supergravity with a single chiral superfield.

In this model, the inflation starts near the inflection point at high scales, and the predictions of inflationary dynamics are consistent with the observations of Planck 2018 [21]. And the inflation will last about 20 e-folding numbers before the inflaton reach the second inflection point at low scales. Since the potential is extremely flat near the inflection point, the inflaton will go through an ultra-slow-roll phase [33–

<sup>a</sup> e-mail: [tjgao@xidian.edu.cn](mailto:tjgao@xidian.edu.cn) (corresponding author)

36], which will cause a large peak in the power spectrum at low scales, which is about seven orders of magnitude higher than the CMB scale power spectrum. When the peak re-enters the horizon, it will induce GWs with the frequency around nanohertz, which can explain the observations of PTA. In addition, when the large peak re-enters the horizon, the high-density regions will collapse into primordial black holes(PBHs) [37–42]. We estimate the abundance of the PBHs, and show that it can be an important component of dark matter.

The paper is organized as follows. In the next section, we setup the double-inflection-point inflationary model in the framework of supergravity. And discuss the inflationary dynamics in Sect. 3. In Sect. 4, we estimate the energy spectrum of induce GWs, and calculate the abundance of PBHs in Sect. 5. The last section is devoted to summary.

### 2 Double-inflection-point inflation from supergravity

In this section, we will construct an inflationary model with double-inflection-point using single chiral superfield in the framework of supergravity. Following Ref. [43], we consider a Kähler potential of the form

$$K = ic(\Phi - \bar{\Phi}) - \frac{1}{2}(\Phi - \bar{\Phi})^2 - \frac{\zeta}{4}(\Phi - \bar{\Phi})^4, \tag{1}$$

with the two constants  $c$  and  $\zeta$  are real. Such Kähler potential satisfies the shift-symmetric  $\Phi \rightarrow \Phi + C$ . The complex field  $\Phi$  can be decomposed into  $(\phi + i\chi)/\sqrt{2}$ , where the real component  $\phi$  is taken as the inflaton. The quartic term with the parameter  $\zeta$  sufficient large is introduced to stabilize the field at  $\langle \chi \rangle \simeq 0$  during inflation.

In order to get a scalar potential which can generate an approximate scale invariant spectrum at CMB scales and induce GWs to explain the PTA signal simultaneously, we consider a superpotential as below

$$W = a_0(1 + a_1e^{-b_1\Phi} + a_2e^{-b_2\Phi} + a_3e^{-b_3\Phi}), \tag{2}$$

where  $a_i$  and  $b_i$  are real constants. Similar potentials with the form of summation of exponential functions have been studied in many works, such as the racetrack model [44–46] or in other models [43]. Here we assume that the SUSY is preserved in vacuum(The small breaking of SUSY in vacuum can be obtained by extending the Kähler potential with a nilpotent superfield, which have been studied in the previous work [25]), which results in the limitation  $W = \partial_\Phi W = 0$ , thus the parameters  $a_1$  and  $a_2$  can be represented by other parameters as

$$a_1 \rightarrow \frac{b_2 + a_3b_2 - a_3b_3}{b_1 - b_2}, a_2 \rightarrow \frac{-b_1 - a_3b_1 + a_3b_3}{b_1 - b_2}. \tag{3}$$

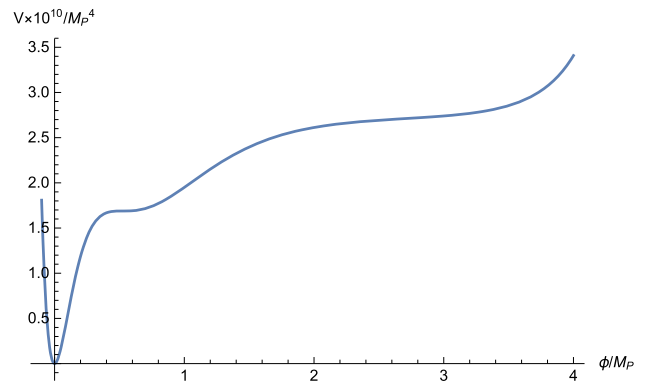


Fig. 1 The scalar potential for the parameter set (7)

Using the superpotential (2) and the Kähler potential (1), we can obtain the scalar potential  $V(\phi)$  by

$$V = e^{K/M_p^2} \left[ D_{\Phi_i} W (K^{-1})^{ij*} D_{\Phi_j} W^* - 3M_p^{-2} |W|^2 \right], \tag{4}$$

where  $D_\Phi$  is defined as

$$D_\Phi W = \partial_\Phi W + M_p^{-2} (\partial_\Phi K) W, \tag{5}$$

and  $(K^{-1})^{ij*}$  is the inverse of the Kähler metric

$$K^{ij*} = \frac{\partial^2 K}{\partial \Phi_i \partial \Phi_j^*}. \tag{6}$$

By choosing the appropriate parameter space, a scalar potential with double-inflection-points can be obtained from the superpotential and Kähler potential above. In the following, we will choose the parameter set below as an example

$$a_0 = 7.695 \times 10^{-6}, \quad a_3 = 1 \times 10^{-6}, \quad c = 2.755, \\ b_1 = 3.5, \quad b_2 = 5.180104, \quad b_3 = -4.08. \tag{7}$$

The corresponding scalar potential is shown in Fig. 1, which contains double-inflection-point.

As we will see in the following discussion, the inflection point at the low energy scales can leads to a large peak in the scalar power spectrum.

### 3 Inflationary dynamics

In the theory of slow-roll inflation, it usually uses the scalar potential  $V$  to define the slow-roll parameters. However, since the potential around the inflection point is extremely flat, when the inflaton meets the second inflection point at low scales, it will go through an ultra-slow-roll phase [33–36]. Therefore, when estimates the power spectrum, we will use the slow-roll parameters defined by the Hubble parameters [47–49],

$$\epsilon_H = -\frac{\dot{H}}{H^2},$$

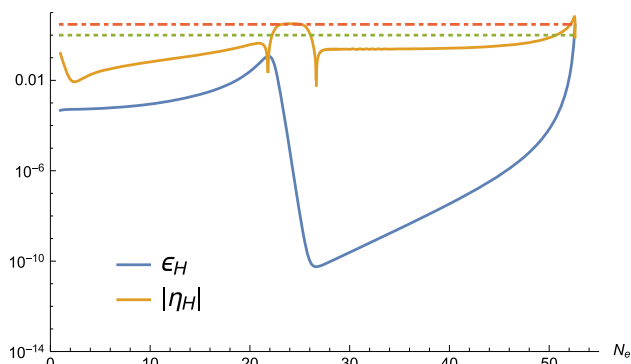


**Fig. 2** The slow-roll parameters  $\epsilon_H$  and  $\eta_H$  with respect to  $N_e$

$$\eta_H = -\frac{\ddot{H}}{2H\dot{H}} = \epsilon_H - \frac{1}{2} \frac{d \ln \epsilon_H}{dN_e}. \tag{8}$$

In Fig. 2, we show the corresponding curves of  $\epsilon_H$  and  $\eta_H$  with respect to the  $e$ -folding numbers  $N_e$ .

As shown in the figure, near the inflection point, the slow-roll parameter  $|\eta_H|$  is greater than 3, which will lead to an ultra-slow-roll phase, and the corresponding curve of parameter  $\epsilon_H$  has a huge valley last more than 30  $e$ -folding numbers, which will lead to a high peak in the power spectrum.

In order to estimate the power spectrum during the ultra-slow-roll phase, we must strictly solve the Mukhanov–Sasaki (MS) equation of mode function [50]

$$\frac{d^2 u_k}{d\tau^2} + \left(k^2 - \frac{1}{z} \frac{d^2 z}{d\tau^2}\right) u_k = 0, \tag{9}$$

where  $\tau$  is the conformal time and  $z \equiv \frac{a}{\mathcal{H}} \frac{d\phi}{d\tau}$ . And then get the power spectrum using

$$\mathcal{P}_{\mathcal{R}} = \frac{k^3}{2\pi^2} \left| \frac{u_k}{z} \right|_{k \ll \mathcal{H}}^2. \tag{10}$$

The numerical results with parameter set (7) are shown in Fig. 3.

As can be seen from the figure, the ultra-slow-roll phase near the inflection point causes a peak in the power spectrum at the low energy scales, which is about seven orders of magnitude higher than the CMB scale spectrum. As we will see below, when this peak re-enters the horizon, it induces GWs with the frequency around nanohertz that can be used to interpret the PTA data.

At the CMB scale, the numerical results shows that the scalar spectral index  $n_s = 1 - 4\epsilon_H + 2\eta_H = 0.9629$ , the tensor-to-scalar ratio  $r = 1 - 4\epsilon_H + 2\eta_H = 0.0087$ , the amplitude of the scalar perturbations  $\ln(10^{10} A_s) = 3.0441$  and the  $e$ -folding numbers during inflation  $N_e = 52.8$ . The results are all consistent with the constraints  $n_s = 0.9649 \pm 0.0042$ ,  $r < 0.064$  and  $\ln(10^{10} A_s) = 3.044 \pm 0.014$  from Planck 2018 [21].

### 4 Gravitational waves induced by scalar perturbations

Since at second order, the tensor perturbations and the scalar perturbations are coupled, so when the scalar perturbations corresponding to the peak of the power spectrum re-enter the horizon, it will induce second-order GWs which can be observed [52–57].

In cosmological perturbation theory, the metric can be expressed under conformal Newtonian gauge as

$$ds^2 = -a^2(1 + 2\Psi)d\eta^2 + a^2 \left[ (1 - 2\Psi)\delta_{ij} + \frac{1}{2}h_{ij} \right] dx^i dx^j, \tag{11}$$

where  $\Psi$  is the scalar perturbations, and the tensor perturbations  $h_{ij}$  can be expanded into Fourier modes by taking the polarization tensors  $e_{ij}^+(\mathbf{k})$  and  $e_{ij}^\times(\mathbf{k})$  as an orthogonal normalized basis

$$h_{ij}(\eta, \mathbf{x}) = \int \frac{d^3 \mathbf{k}}{(2\pi)^{3/2}} e^{i\mathbf{k}\cdot\mathbf{x}} \left[ h_{\mathbf{k}}^+(\eta) e_{ij}^+(\mathbf{k}) + h_{\mathbf{k}}^\times(\eta) e_{ij}^\times(\mathbf{k}) \right]. \tag{12}$$

Then the second order equation of motion of tensor modes  $h_{\mathbf{k}}(\eta)$  can be written as

$$h_{\mathbf{k}}''(\eta) + 2\mathcal{H}h_{\mathbf{k}}'(\eta) + k^2 h_{\mathbf{k}}(\eta) = S_{\mathbf{k}}(\eta), \tag{13}$$

where we have omitted the polarization index for simplicity. And  $S_{\mathbf{k}}(\eta)$  on the right-hand side of the equation is the source term in the Fourier space, which is given by

$$S_{\mathbf{k}}(\eta) = 4 \int \frac{d^3 p}{(2\pi)^{3/2}} e_{ij}(\mathbf{k}) p_i p_j \times \left( 2\Psi_{\mathbf{p}} \Psi_{\mathbf{k}-\mathbf{p}} + \frac{4}{3(1+w)\mathcal{H}^2} (\Psi'_{\mathbf{p}} + \mathcal{H}\Psi_{\mathbf{p}}) \times (\Psi'_{\mathbf{k}-\mathbf{p}} + \mathcal{H}\Psi_{\mathbf{k}-\mathbf{p}}) \right). \tag{14}$$

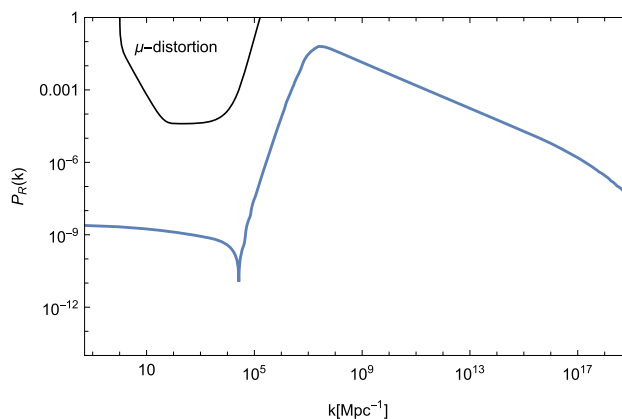


**Fig. 3** The numerical results of the primordial power spectrum of scalar perturbations. And the upper bound is the  $\mu$ -distortion for the steepest growth  $k^4$  power spectrum [51]

If the mode corresponds to the peak that re-enter the horizon during the radiation dominated(RD) era, the equation of state in the above is taken  $\omega = 1/3$ , and the energy spectrum of the GWs can be expressed in terms of the oscillation average of tensor power spectrum as

$$\Omega_{\text{GW}}(\eta, k) = \frac{1}{24} \left( \frac{k}{\mathcal{H}} \right)^2 \overline{\mathcal{P}_h(\eta, k)}. \tag{15}$$

Using the Green’s function method, and sum the two polarization modes of GWs, one finally gets the expression of the GW energy spectrum as follows

$$\begin{aligned} \Omega_{\text{GW}}(\eta, k) &= \frac{1}{12} \int_0^\infty dv \int_{|1-v|}^{1+v} du \\ &\times \left( \frac{4v^2 - (1 + v^2 - u^2)^2}{4uv} \right)^2 \mathcal{P}_{\mathcal{R}}(ku) \mathcal{P}_{\mathcal{R}}(kv) \\ &\times \left( \frac{3}{4u^3v^3} \right)^2 (u^2 + v^2 - 3)^2 \\ &\times \left\{ \left[ -4uv + (u^2 + v^2 - 3) \ln \left| \frac{3 - (u + v)^2}{3 - (u - v)^2} \right| \right]^2 \right. \\ &\left. + \pi^2 (u^2 + v^2 - 3)^2 \Theta(u + v - \sqrt{3}) \right\}, \tag{16} \end{aligned}$$

where  $u \equiv |\mathbf{k} - \mathbf{p}|/k$ ,  $v \equiv |\mathbf{p}|/k$  and  $x \equiv k\eta$  are three dimensionless variables [58].

Using the energy spectrum above produced in the RD period, one can get the current spectrum  $\Omega_{\text{GW},0}$  using [54]

$$\Omega_{\text{GW},0} = 0.83 \left( \frac{g_{*,0}}{g_{*,p}} \right)^{-1/3} \Omega_{r,0} \Omega_{\text{GW}}, \tag{17}$$

with the density fraction of radiation at the present time is  $\Omega_{r,0} \simeq 9.1 \times 10^{-5}$ , and the effective degrees of freedom at the present time is  $g_{*,0} \simeq 106.75$ , and when the peak mode crosses the horizon is  $g_{*,p} \simeq 10.75$ .

Combine expressions (16), (17) and the power spectrum  $\mathcal{P}_{\mathcal{R}}$  obtained in the previous section, we calculate the GW energy spectrum at the present time numerically, and show the result in Fig. 4, with the horizontal axis is the frequency

$$f \approx 0.03 \text{ Hz} \frac{k}{2 \times 10^7 \text{ pc}^{-1}}. \tag{18}$$

The expected sensitivity curves for some current and planned detectors such as LISA, EPTA, etc. are also shown there [59–64]. Recently, the worldwide PTA collaborations found strong evidence for the existence of SGWB [1–8], and the constraints of NANOGrav and EPTA are also shown in Fig. 4.

We can see that the frequency of the peak of GW spectrum predicted by the model is around nanohertz, and the curves can explain the PTA data.

### 5 Production of primordial black holes

When the peak of the power spectrum re-enters the horizon, if the amplitude of fluctuations is significantly large, the high-density region can cause gravitational collapse, thus, form PBHs. Assuming that the mass of the resulting PBHs is proportional to the horizon mass when re-entry, and it can be approximately written as [65,66]

$$\begin{aligned} M &= \gamma \frac{4}{3} \pi \rho H^{-3} \simeq 10^{-13} M_\odot \left( \frac{\gamma}{0.2} \right) \left( \frac{g_*}{106.75} \right)^{-1/6} \\ &\times \left( \frac{k}{4.9 \times 10^{12} \text{ Mpc}^{-1}} \right)^{-2}, \tag{19} \end{aligned}$$

where  $\gamma$  is the parameter related to the details of gravitational collapse, and we take  $\gamma \sim 0.2$  here [67].

Using the Press–Schechter model of gravitational collapse, and assuming the density perturbations are Gaussian, the proportion of the PBH mass to the overall energy density during its formation period is given by

$$\beta(M) \equiv \frac{\rho_{\text{PBH}}(M)}{\rho_{\text{tot}}} = \frac{1}{2} \text{erfc} \left( \frac{\delta_c}{\sqrt{2\sigma^2(M)}} \right), \tag{20}$$

where we choose the threshold for collapse as  $\delta_c \simeq 0.45$  [68,69], and  $\sigma^2(M)$  is the variance of the comoving density perturbations, which is evaluated as

$$\sigma^2(M(k)) = \frac{16}{81} \int d \ln q (q/k)^4 P_{\mathcal{R}}(q) W(q/k)^2, \tag{21}$$

with the Gaussian window function  $W(x) = \exp(-x^2/2)$ . The present fractional abundance of PBHs in the DM is [65, 70].

$$\frac{\Omega_{\text{PBH}}}{\Omega_{\text{DM}}} = \int f(M) d \ln M, \tag{22}$$

with

$$\begin{aligned} f(M) &\simeq \left( \frac{\beta(M)}{1.04 \times 10^{-14}} \right) \left( \frac{\gamma}{0.2} \right)^{3/2} \\ &\times \left( \frac{g_*}{106.75} \right)^{-1/4} \left( \frac{0.12}{\Omega_{\text{DM}} h^2} \right) \left( \frac{M}{10^{-13} M_\odot} \right)^{-1/2}. \tag{23} \end{aligned}$$

The numerical results of PBHs production show that in the model the peak mass of the PBHs is  $M_{\text{PBHs}}^{\text{peak}} = 3.288 \times 10^{-3} M_\odot$ , the corresponding abundance is  $\Omega_{\text{PBH}}/\Omega_{\text{DM}} = 1.960 \times 10^{-3}$ , which can be an important component of DM. The corresponding results and the observational constraints from Ref. [71] are shown in Fig. 5.

### 6 Summary

In this paper, we try to explain the PTA data in the framework of supergravity using a single chiral superfield. Con-

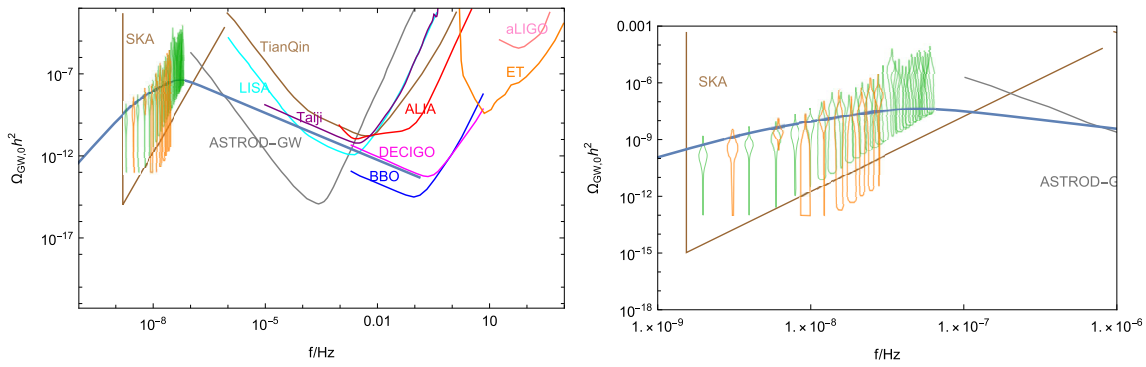


**Fig. 4** The numerical results of the energy spectrum of GWs at the present time predicted by the model. The expected sensitivity curves for some current or planned detectors are also shown in the upper part

[59–64]. The orange region shows the data of EPTA [2,3] and the green region shows the PTA data of NANOGrav [4,5]. The panel on the right is a partial enlargement

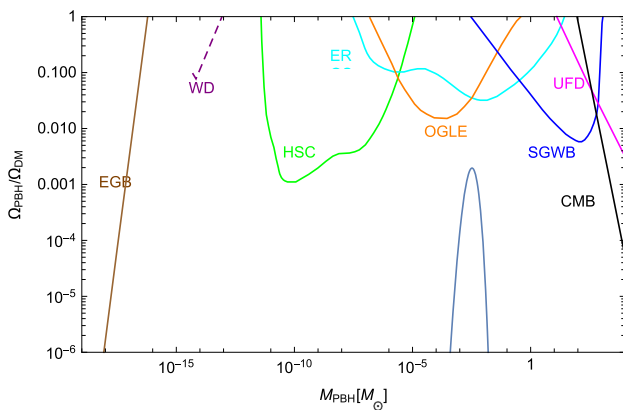


**Fig. 5** The abundance of PBHs. The curves in the upper part are the observational constraints [71]

considering a shift symmetry Kähler potential and an exponential superpotential with three terms, we obtain an inflationary potential with double-inflection-point by choosing the appropriate parameter space (In order to explain the observations, the model parameters need to be finely tuned. So if one add higher order terms, although a similar double-inflection-point potential can still be obtained, the parameter space needs to be changed). In this model, the inflation starts near the first inflection point, and the predictions at the CMB scale are in agreement with Planck 2018. After a little more than 20 e-folding numbers, the inflaton reaches the second inflection point and undergoes an ultra-slow-roll phase, which will result in a large peak in the power spectrum. When this peak re-enters the horizon, it will induce gravitational waves with the frequency around nanohertz, thus can explain the PTA data. At the same time, the high-density regions corresponding to the peak when re-entering the horizon will collapse into planet-mass PBHs. The numerical results show that the peak mass is about  $3.288 \times 10^{-3} M_{\odot}$ , and the corresponding abundance is about  $1.960 \times 10^{-3}$ , which can be an important component of DM.

**Acknowledgements** This work was supported by “the National Natural Science Foundation of China” (NNSFC) with Grant No. 11705133, and by “the Natural Science Basic Research Program of Shaanxi Province” No. 2023-JC-YB-072. KSS is supported by “the Natural Science Foundation of Hebei Province” under Grants No. A2022104001. XYY is supported by “Department of Education of Liaoning Province” with Grant No. JYTMS20230937.

**Data Availability Statement** This manuscript has no associated data or the data will not be deposited. [Authors’ comment: This is a theoretical study and the results can be obtained explicitly from the relevant calculations presented in this paper.]

**Open Access** This article is licensed under a Creative Commons Attribution 4.0 International License, which permits use, sharing, adaptation, distribution and reproduction in any medium or format, as long as you give appropriate credit to the original author(s) and the source, provide a link to the Creative Commons licence, and indicate if changes were made. The images or other third party material in this article are included in the article’s Creative Commons licence, unless indicated otherwise in a credit line to the material. If material is not included in the article’s Creative Commons licence and your intended use is not permitted by statutory regulation or exceeds the permitted use, you will need to obtain permission directly from the copyright holder. To view a copy of this licence, visit <http://creativecommons.org/licenses/by/4.0/>.

Funded by SCOAP<sup>3</sup>.

**References**

1. H. Xu, S. Chen, Y. Guo, J. Jiang, B. Wang, J. Xu, Z. Xue, R.N. Caballero, J. Yuan, Y. Xu et al., Res. Astron. Astrophys. **23**(7), 075024 (2023). <https://doi.org/10.1088/1674-4527/acdfa5>. [arXiv:2306.16216](https://arxiv.org/abs/2306.16216) [astro-ph.HE]
2. J. Antoniadis et al. [EPTA], Astron. Astrophys. **678**, A48 (2023). [arXiv:2306.16224](https://arxiv.org/abs/2306.16224) [astro-ph.HE]
3. J. Antoniadis et al. [EPTA and InPTA:], Astron. Astrophys. **678**, A50 (2023). <https://doi.org/10.1051/0004-6361/202346844>. [arXiv:2306.16214](https://arxiv.org/abs/2306.16214) [astro-ph.HE]
4. G. Agazie et al. [NANOGrav], Astrophys. J. Lett. **951**(1), L8 (2023). [arXiv:2306.16213](https://arxiv.org/abs/2306.16213) [astro-ph.HE]
5. G. Agazie et al. [NANOGrav], Astrophys. J. Lett. **951**(1), L9 (2023). [arXiv:2306.16217](https://arxiv.org/abs/2306.16217) [astro-ph.HE]

6. A. Afzal et al. [NANOGrav], *Astrophys. J. Lett.* **951**(1), L11 (2023). <https://doi.org/10.3847/2041-8213/acdc91>. [arXiv:2306.16219](https://arxiv.org/abs/2306.16219) [astro-ph.HE]
7. A. Zic, D.J. Reardon, A. Kapur, G. Hobbs, R. Mandow, M. Curyło, R.M. Shannon, J. Askew, M. Bailes, N.D.R. Bhat, et al., [arXiv:2306.16230](https://arxiv.org/abs/2306.16230) [astro-ph.HE]
8. D.J. Reardon, A. Zic, R.M. Shannon, G.B. Hobbs, M. Bailes, V. Di Marco, A. Kapur, A.F. Rogers, E. Thrane, J. Askew et al., *Astrophys. J. Lett.* **951**(1), L6 (2023). <https://doi.org/10.3847/2041-8213/acdd02>. [arXiv:2306.16215](https://arxiv.org/abs/2306.16215) [astro-ph.HE]
9. R.W. Hellings, G.S. Downs, *Astrophys. J. Lett.* **265**, L39–L42 (1983). <https://doi.org/10.1086/183954>
10. A. Ashoorioon, K. Rezaadeh, A. Rostami, *Phys. Lett. B* **835**, 137542 (2022). [arXiv:2202.01131](https://arxiv.org/abs/2202.01131) [astro-ph.CO]
11. S. He, L. Li, S. Wang, S.J. Wang, [arXiv:2308.07257](https://arxiv.org/abs/2308.07257) [hep-ph]
12. K.T. Abe, Y. Tada, *Phys. Rev. D* **108**(10), L101304 (2023). [arXiv:2307.01653](https://arxiv.org/abs/2307.01653) [astro-ph.CO]
13. J. Garcia-Bellido, E. Ruiz Morales, *Phys. Dark Univ.* **18**, 47 (2017). [arXiv:1702.03901](https://arxiv.org/abs/1702.03901) [astro-ph.CO]
14. C. Germani, T. Prokopec, *Phys. Dark Univ.* **18**, 6–10 (2017). [arXiv:1706.04226](https://arxiv.org/abs/1706.04226) [astro-ph.CO]
15. H. Di, Y. Gong, *JCAP* **1807**(07), 007 (2018). [arXiv:1707.09578](https://arxiv.org/abs/1707.09578) [astro-ph.CO]
16. G. Ballesteros, M. Taoso, *Phys. Rev. D* **97**(2), 023501 (2018). [arXiv:1709.05565](https://arxiv.org/abs/1709.05565)
17. I. Dalianis, A. Kehagias, G. Tringas, *JCAP* **1901**, 037 (2019). [arXiv:1805.09483](https://arxiv.org/abs/1805.09483) [astro-ph.CO]
18. A. Ashoorioon, A. Rostami, J.T. Firouzjaee, *JHEP* **07**, 087 (2021). [arXiv:1912.13326](https://arxiv.org/abs/1912.13326) [astro-ph.CO]
19. O. Özsoy, S. Parameswaran, G. Tasinato, I. Zavala, *JCAP* **07**, 005 (2018). <https://doi.org/10.1088/1475-7516/2018/07/005>. [arXiv:1803.07626](https://arxiv.org/abs/1803.07626) [hep-th]
20. G. Hinshaw et al., WMAP Collaboration, *Astrophys. J. Suppl.* **208**, 19 (2013). [arXiv:1212.5226](https://arxiv.org/abs/1212.5226)
21. Y. Akrami et al. [Planck Collaboration], [arXiv:1807.06211](https://arxiv.org/abs/1807.06211) [astro-ph.CO]
22. D.Z. Freedman, P. van Nieuwenhuizen, S. Ferrara, *Phys. Rev. D* **13**, 3214 (1976)
23. S. Deser, B. Zumino, *Phys. Lett. B* **62**, 335 (1976)
24. J. Wess, J. Bagger, *Supersymmetry and Supergravity*, 2nd edn. (Princeton University Press, Princeton, 1992)
25. T.J. Gao, Z.K. Guo, *Phys. Rev. D* **91**, 123502 (2015). [arXiv:1503.05643](https://arxiv.org/abs/1503.05643) [hep-th]
26. T.J. Gao, W.T. Xu, X.Y. Yang, *Mod. Phys. Lett. A* **32**(2), 1750072 (2017). [arXiv:1606.05951](https://arxiv.org/abs/1606.05951) [hep-ph]
27. T.J. Gao, Z.K. Guo, *Phys. Rev. D* **98**(6), 063526 (2018). [arXiv:1806.09320](https://arxiv.org/abs/1806.09320) [hep-ph]
28. Supergravity based inflation models: a review. [arXiv:1101.2488](https://arxiv.org/abs/1101.2488)
29. M. Kawasaki, M. Yamaguchi, T. Yanagida, Natural chaotic inflation in supergravity. *Phys. Rev. Lett.* **85**, 3572–3575 (2000). [arXiv:hep-ph/0004243](https://arxiv.org/abs/hep-ph/0004243)
30. M. Kawasaki, M. Yamaguchi, T. Yanagida, Natural chaotic inflation in supergravity and leptogenesis. *Phys. Rev. D* **63**, 103514 (2001). [arXiv:hep-ph/0011104](https://arxiv.org/abs/hep-ph/0011104)
31. S.V. Ketov, T. Terada, Inflation in supergravity with a single chiral superfield. *Phys. Lett. B* **736**, 272–277 (2014). [arXiv:1406.0252](https://arxiv.org/abs/1406.0252)
32. S.V. Ketov, T. Terada, On SUSY Restoration in Single-Superfield Inflationary Models of Supergravity. *Eur. Phys. J. C* **76**(8), 438 (2016). [arXiv:1606.02817](https://arxiv.org/abs/1606.02817)
33. C. Germani, T. Prokopec, *Phys. Dark Univ.* **18**, 6 (2017). [arXiv:1706.04226](https://arxiv.org/abs/1706.04226) [astro-ph.CO]
34. K. Dimopoulos, *Phys. Lett. B* **775**, 262 (2017). [arXiv:1707.05644](https://arxiv.org/abs/1707.05644) [hep-ph]
35. J.M. Ezquiaga, J. García-Bellido, *JCAP* **1808**, 018 (2018). [arXiv:1805.06731](https://arxiv.org/abs/1805.06731) [astro-ph]
36. D. Cruces, C. Germani, T. Prokopec, *JCAP* **1903**(03), 048 (2019). [arXiv:1807.09057](https://arxiv.org/abs/1807.09057) [gr-qc]
37. J. Yokoyama, *Astron. Astrophys.* **318**, 673 (1997). [arXiv:astro-ph/9509027](https://arxiv.org/abs/astro-ph/9509027)
38. J. Garcia-Bellido, A.D. Linde, D. Wands, *Phys. Rev. D* **54**, 6040 (1996). [arXiv:astro-ph/9605094](https://arxiv.org/abs/astro-ph/9605094)
39. S. Clesse, J. Garcia-Bellido, *Phys. Rev. D* **92**(2), 023524 (2015). [arXiv:1501.07565](https://arxiv.org/abs/1501.07565) [astro-ph.CO]
40. J. Garcia-Bellido, M. Peloso, C. Unal, *JCAP* **1612**(12), 031 (2016). [arXiv:1610.03763](https://arxiv.org/abs/1610.03763) [astro-ph.CO]
41. S.L. Cheng, W. Lee, K.W. Ng, *JHEP* **1702**, 008 (2017). [https://doi.org/10.1007/JHEP02\(2017\)008](https://doi.org/10.1007/JHEP02(2017)008). [arXiv:1606.00206](https://arxiv.org/abs/1606.00206) [astro-ph.CO]
42. C. Fu, P. Wu, H. Yu, [arXiv:1907.05042](https://arxiv.org/abs/1907.05042) [astro-ph.CO]
43. S.V. Ketov, T. Terada, On SUSY restoration in single-superfield inflationary models of supergravity. *Eur. Phys. J. C* **76**(8), 438 (2016). [arXiv:1606.02817](https://arxiv.org/abs/1606.02817)
44. J.J. Blanco-Pillado, C.P. Burgess, J.M. Cline et al., Racetrack inflation. *JHEP* **0411**, 063 (2004)
45. C. Escoda, M. Gomez-Reino, F. Quevedo, Saltatory de Sitter string vacua. *JHEP* **11**, 065 (2003). [arXiv:hep-th/0307160](https://arxiv.org/abs/hep-th/0307160)
46. N.V. Krasnikov, On supersymmetry breaking in superstring theories. *Phys. Lett. B* **193**, 37 (1987)
47. D.J. Schwarz, C.A. Terrero-Escalante, A.A. Garcia, *Phys. Lett. B* **517**, 243 (2001). [arXiv:astro-ph/0106020](https://arxiv.org/abs/astro-ph/0106020)
48. S.M. Leach, A.R. Liddle, J. Martin, D.J. Schwarz, *Phys. Rev. D* **66**, 023515 (2002). [arXiv:astro-ph/0202094](https://arxiv.org/abs/astro-ph/0202094)
49. D.J. Schwarz, C.A. Terrero-Escalante, *JCAP* **0408**, 003 (2004). [arXiv:hep-ph/0403129](https://arxiv.org/abs/hep-ph/0403129)
50. G. Ballesteros, M. Taoso, *Phys. Rev. D* **97**(2), 023501 (2018). [arXiv:1709.05565](https://arxiv.org/abs/1709.05565)
51. C.T. Byrnes, P.S. Cole, S.P. Patil, *JCAP* **06**, 028 (2019). <https://doi.org/10.1088/1475-7516/2019/06/028>. [arXiv:1811.11158](https://arxiv.org/abs/1811.11158) [astro-ph.CO]
52. D. Baumann, P.J. Steinhardt, K. Takahashi, K. Ichiki, *Phys. Rev. D* **76**, 084019 (2007). [arXiv:hep-th/0703290](https://arxiv.org/abs/hep-th/0703290)
53. K.N. Ananda, C. Clarkson, D. Wands, *Phys. Rev. D* **75**, 123518 (2007). [arXiv:gr-qc/0612013](https://arxiv.org/abs/gr-qc/0612013)
54. K. Ando, K. Inomata, M. Kawasaki, K. Mukaida, T.T. Yanagida, *Phys. Rev. D* **97**(12), 123512 (2018). [arXiv:1711.08956](https://arxiv.org/abs/1711.08956) [astro-ph.CO]
55. H. Kodama, M. Sasaki, *Prog. Theor. Phys. Suppl.* **78**, 1 (1984)
56. V.F. Mukhanov, H.A. Feldman, R.H. Brandenberger, *Phys. Rep.* **215**, 203 (1992)
57. J.R. Espinosa, D. Racco, A. Riotto, *JCAP* **09**, 012 (2018). [arXiv:1804.07732](https://arxiv.org/abs/1804.07732) [hep-ph]
58. K. Kohri, T. Terada, *Phys. Rev. D* **97**(12), 123532 (2018). [arXiv:1804.08577](https://arxiv.org/abs/1804.08577) [gr-qc]
59. H. Audley et al., [arXiv:1702.00786](https://arxiv.org/abs/1702.00786) [astro-ph.IM]
60. Z.K. Guo, R.G. Cai, Y.Z. Zhang, [arXiv:1807.09495](https://arxiv.org/abs/1807.09495) [gr-qc]
61. C.J. Moore, R.H. Cole, C.P.L. Berry, *Class. Quantum Gravity* **32**(1), 015014 (2015). [arXiv:1408.0740](https://arxiv.org/abs/1408.0740) [gr-qc]
62. J. Luo et al. [TianQin Collaboration], *Class. Quantum Gravity* **33**(3), 035010 (2016). [arXiv:1512.02076](https://arxiv.org/abs/1512.02076) [astro-ph.IM]
63. K. Kuroda, W.T. Ni, W.P. Pan, *Int. J. Mod. Phys. D* **24**(14), 1530031 (2015). [arXiv:1511.00231](https://arxiv.org/abs/1511.00231) [gr-qc]
64. M. Drees, Y. Xu, [arXiv:1905.13581](https://arxiv.org/abs/1905.13581) [hep-ph]
65. K. Inomata, M. Kawasaki, K. Mukaida, T.T. Yanagida, *Phys. Rev. D* **97**(4), 043514 (2018). <https://doi.org/10.1103/PhysRevD.97.043514>. [arXiv:1711.06129](https://arxiv.org/abs/1711.06129) [astro-ph.CO]
66. G. Ballesteros, M. Taoso, Primordial black hole dark matter from single field inflation. *Phys. Rev. D* **97**, 023501 (2018)
67. B.J. Carr, The primordial black hole mass spectrum. *Astrophys. J.* **201**, 1 (1975)
68. I. Musco, J.C. Miller, Primordial black hole formation in the early universe: critical behaviour and self-similarity. *Class. Quantum Gravity* **30**, 145009 (2013)

69. T. Harada, C.-M. Yoo, K. Kohri, Threshold of primordial black hole formation. *Phys. Rev. D* **88**, 084051 (2013) [Erratum, *Phys. Rev. D* **89**, 029903(E) (2014)]
70. P.A.R. Ade et al., Planck 2015 results. XIII. Cosmological parameters. *Astron. Astrophys.* **594**, A13 (2016)
71. M.P. Hertzberg, M. Yamada, *Phys. Rev. D* **97**, 083509 (2018). [arXiv:1712.09750](https://arxiv.org/abs/1712.09750) [astro-ph.CO]